Received: 25 July 2022 | Revised: 10 December 2022 | Accepted: 5 January 2023

https://doi.org/10.1016/j.jtha.2023.01.007

ORIGINAL ARTICLE

Acidification of blood plasma facilitates the separation and analysis of extracellular vesicles

Danilo Mladenović[1,2] | Delaram Khamari[3,4] | Ágnes Kittel[5] | Kairi Koort[2] | Edit I. Buzás[3,4,6] | Nataša Zarovni[1,7]

[1]HansaBioMed Life Sciences Ltd., Tallinn, Estonia

[2]School of Natural Sciences and Health, Tallinn University, Tallinn, Estonia

[3]Department of Genetics, Cell- and Immunobiology, Semmelweis University, Budapest, Hungary

[4]Eötvös Loránd Research Network, Translational Extracellular Vesicle Research Group, Semmelweis University, Budapest, Hungary

[5]Eötvös Loránd Research Network, Institute of Experimental Medicine, Budapest, Hungary

[6]Hungarian Center of Excellence Molecular Medicine, Extracellular Vesicle Research Group, Semmelweis University, Budapest, Hungary

[7]Exosomics SpA, Siena, Italy

Correspondence
Nataša Zarovni, HansaBioMed Life Sciences Ltd., Mäealuse 2/1, 12618 Tallinn, Estonia.
Email: nzarovni@exosomics.eu

Funding information

This work was supported by following funding programs: European Union's Horizon 2020 research and innovation program under the grant agreement number H2020-MSCA-ITN-2017-722148 (TRAIN EV); European Regional Development Fund Enterprise Estonia's Applied Research Program under the grant agreement number 2014-2020.4.02.21-0398 (EVREM), National Scientific Research Program of Hungary (OTKA) NVKP_16-1-2016- 0017, Higher Education Institutional Excellence

Abstract

Background: Blood plasma is available with minimal invasive sampling, it has significant diagnostic utility, and it is a valuable source of extracellular vesicles (EVs). Nevertheless, rich protein content, the presence of lipoproteins (LPs) that share similar biophysical properties, and relatively low abundance of EVs, especially those of rare subpopulations, make any downstream application a very challenging task. The growing evidence of the intricate surface interactome of EVs, and the association of EVs with LPs, impose further challenges during EV purification, detection, and biomarker analyses.

Objectives: In this study, we tackled the fundamental issues of plasma EV yield and LP co-isolation and their implications in the subsequent marker analyses.

Methods: Moderate acidification of plasma was combined with size exclusion chromatography (SEC) and/or differential centrifugation (DC) to disrupt LPs and improve recovery of EVs and their subsequent detection by immunoassays and single-particle analysis methods.

Results: Our results demonstrate a surprisingly efficient enrichment of EVs (up to 3.3-fold higher than at pH 7) and partial depletion of LPs (up to 61.2%). Acidification of blood plasma samples enabled a quick single-step isoelectric precipitation of up to 20.4% of EVs directly from plasma, upon short low-speed centrifugation.

Conclusion: Thus, acidification holds potential as a simple and inexpensive methodological step, which improves the efficacy of plasma EV enrichment and may have implications in future biomarker discoveries.

KEYWORDS
blood plasma, extracellular vesicles, immunoassay, lipoproteins, pH

Manuscript handled by: Patricia Liaw

Final decision: Patricia Liaw, 05 January 2023

Danilo Mladenović and Delaram Khamari contributed equally to this study.

Program – Therapeutic development, Ministry for National Economy of Hungary under the grant number VEKOP-2.3.2-16-2016-00002, VEKOP-2.3.3-15-2017-00016, European Union's Horizon 2020 research and innovation program under the grant agreement number 739593, and the grant TKP-2021-Terapias-EGA-23.

1 | INTRODUCTION

Multitude of different extracellular vesicles (EVs) can be found in bodily fluids [1–5], all of which are appealing substrates for liquid biopsy, thus enabling the exploration of EVs' potential in non-invasive diagnostics [6–11]. Still, the intricate milieu of these biofluids aggravates the adequate enrichment and detection of relevant EV markers. Blood carries heterogeneous population of EVs, although the vast majority is released by blood cells, whereas only a small fraction represents other tissues and cells [12]. On top of that, lipoproteins (LPs) that have similar biophysical properties (size, shape, and density) are outnumbering EVs by orders of magnitude [13–15]. Noteworthy, it is reported that LPs themselves can carry markers of clinical relevance which can further hamper the identification and correct attribution of true vesicular markers [16–18]. Therefore, finding a way to enrich plasma EVs, or deplete LPs, is highly desirable, yet challenging task. Additional layer of complexity to the already challenging purification processes is posed by the intricate and intimate surface interactome of EVs and other extracellular components, including LPs, as a result of potential nonspecific and specific interactions [19–21].

It has been previously reported that LPs, especially VLDL particles, are sensitive to mildly acidic environments and get destabilized and disintegrated at pH lower than 6 [22]. One of the major protein components of many LPs, ApoB was also reported to undergo structural remodeling due to its instability when lowering the pH [23]. On the contrary, the effect of acidification on plasma EVs is insufficiently explored, yet, it holds potential as a technique for isoelectric precipitation, given that EVs have net negative surface charge [24,25].

In this study, we strived to leverage the pH modification as a mean of plasma EV enrichment along with LP disruption and depletion, in order to meet the need for a robust, yet undemanding preparation method. Such a step is a critical prerequisite of EV-associated biomarker discovery, prior to proceeding with the development and validation of EV-based diagnostics tools. A particular problem is the detection of rare EV populations that are greatly underrepresented in circulation, although they are still likely to hold a major clinical relevance for early-stage disease diagnostics. Hereby, we evaluated the effect of moderate acidification (pH 6.0 to pH 5.0) on EV isolation from human blood plasma; we studied its impact on LPs co-isolation and its implications in downstream analysis and biomarker discovery.

Essentials

- Plasma-derived extracellular vesicles (EVs) are scarce and co-isolate with lipoproteins (LPs).
- Unlike EVs, LPs are sensitive to mildly acidic conditions.
- Acidification enriches plasma EVs via isoelectric precipitation and partially depletes LPs.
- Quick EV enrichment via acidification may facilitate future biomarker research.

2 | RESULTS

2.1 | Plasma acidification improves the recovery of EVs both in SEC and DC

In order to establish the optimal pH condition for isolation and detection of plasma EVs, while also monitoring the effect it has on LPs and their co-purification with EVs, we have assessed a moderate acidic environment at multiple pH values in the range from pH 7 to pH 5 (i.e., pH 7, 6, 5.5, and 5). Upon acidification, the resulting precipitates (P6, P5.5, and P5) were separated from the rest of the plasma with a short low-speed centrifugation (5 minutes at 300 *g*) (Figure 1A). As there was no precipitate in the control pH 7 sample, the same amount of plasma from the bottom of the tube was taken as the P7. The obtained precipitate-depleted plasma samples (PDP7, PDP6, PDP5.5, and PDP5) were purified with SEC. Automated western blot analyses of pooled EV SEC fractions from 7 to 11 (SEC7, SEC6, SEC5.5, and SEC5) showed that EV marker CD9 was the most abundant at pH 5.5 (Figure 1B, left). At the same time, the band intensity of LP marker ApoA1 indicated pH dependence, being the highest at pH 5 (Figure 1B, right). The acidification-induced precipitation was more prominent the lower the pH was. This was reflected in the content of the EV marker, as the signal was the highest in P5.5 and P5 (Figure 1C, left). The same was observed with LP marker ApoA1 (Figure 1C, right). Given that the yield of EV marker in SEC samples was the highest at pH 5.5, with the EV:LP ratio providing the optimal tradeoff (Figure 1B), we opted for pH 5.5 as the condition for further assessment of plasma EVs recovery.

PDP5.5 purified by SEC at pH 5.5 showed a higher signal of CD9 in sandwich enzyme-linked immunosorbent assay (ELISA), compared with a control PDP7 purified at pH 7 (Figure 1D). On the contrary,

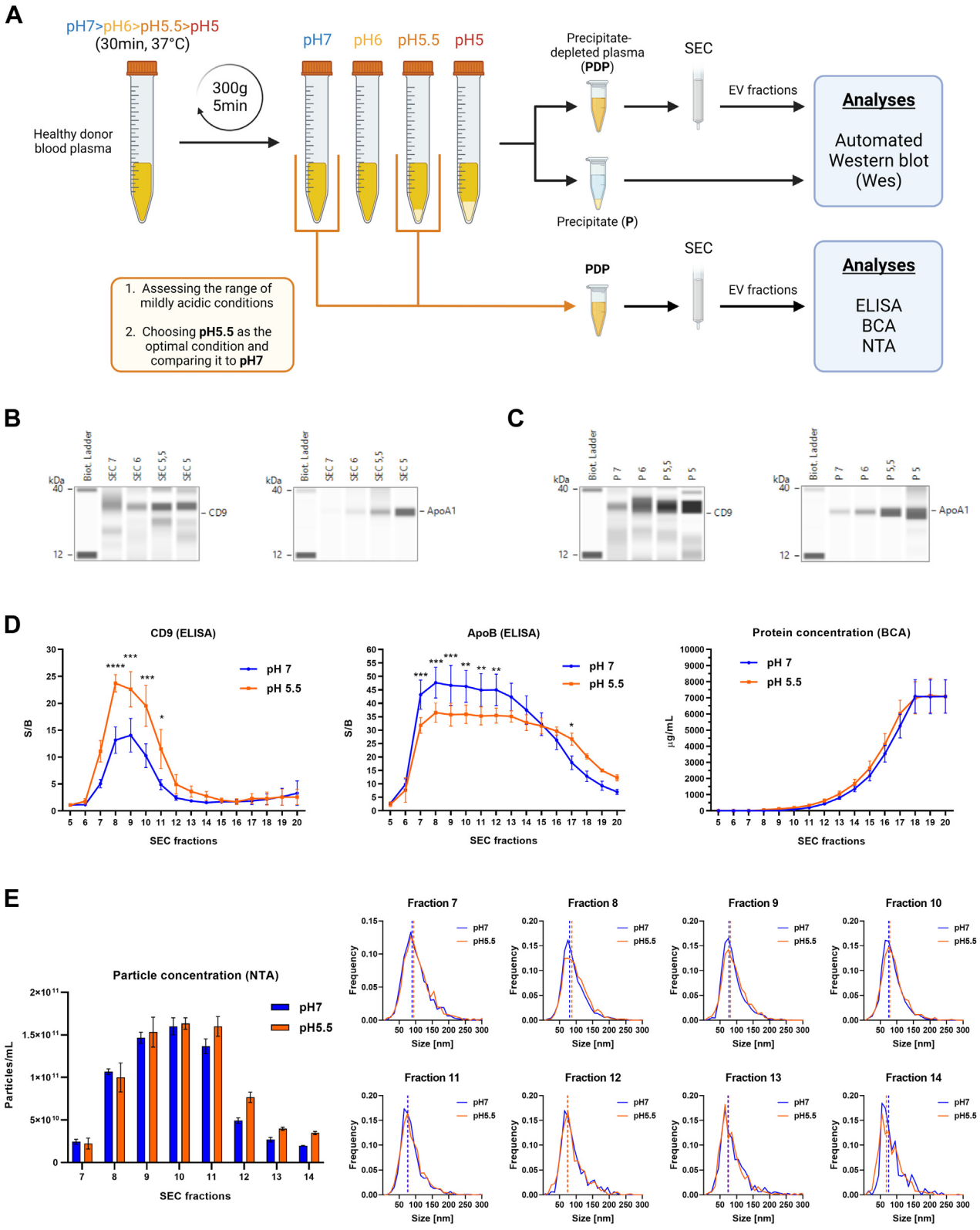

FIGURE 1 Assessing the effect of multiple pH conditions on EV purification and downstream analysis. **(A)** Healthy donor plasma samples were subjected to moderate acidification (pH 5 to pH 7) using 1-M HCl. P samples were separated and PDP samples were further purified with SEC. **(B)** Pooled fractions containing EVs (SEC) and **(C)** P samples from all pH conditions (pH 5, 5.5, 6, and 7) were analyzed using an automated western blot system (Protein Simple Wes) for the expression of common EV marker CD9 and LP marker ApoA1. Upon choosing pH 5.5 as the optimal condition for the recovery of EVs, **(D)** individual SEC fractions were further analyzed for EV marker expression using a sandwich ELISA (anti-CD9 antibody for capturing and detection), and LP marker expression using an indirect ELISA (high-binding capacity 96-well plate for

ApoB signal was significantly reduced in all of the fractions containing EVs, while the total protein content showed a mild but statistically insignificant elevation (Figure 1D). The initial results raised a concern that potential protein contamination could contribute to the increase of the CD9 ELISA signal. However, this hypothesis was rejected as the later SEC fractions (15-20) showed comparably low CD9 signal even though they had significantly higher protein content. Furthermore, sandwich ELISA relies on the concomitant expression of multiple CD9 molecules per analyte (i.e., one for capturing and one for detection), thus, reaffirming that the signal is indeed coming from EVs. Particle concentration and size distribution (PSD) in both pH conditions were comparable, whereas there was a slight shift in the median size toward the larger diameters in most of the EV SEC fractions at pH 5.5 (Figure 1E).

The effect of plasma acidification on the recovery of EVs by 2 different methods, either differential centrifugation (DC) alone, or SEC purification of PDP5.5 followed by DC of pooled EV SEC fractions (Figure 2A), was further assessed by analysis of CD9 and CD63 expression with flow cytometry (Figure 2B). No significant differences were observed in the 20 500-*g* pellet of pooled EV SEC fractions at pH 5.5 (20k SEC5.5) compared with the control sample at pH 7 (20k SEC7), whereas slight enrichment of both EV markers was observed in 20 500 *g* pellet from PDP at pH 5.5 (20k PDP5.5) compared with the control (20k PDP7). The most prominent effect of acidification was seen in 20 500 *g* pellet of P5.5 (20k P5.5) that had 6- to 7-fold higher signal for both CD9 and CD63, compared with a pH 7 control (20k P7). Further on, after 100 000 *g* centrifugation, the signal of 2 markers was significantly higher both in pellet of pooled EV SEC fractions and in pellet of PDP (100k SEC5.5 and 100k PDP5.5, respectively), reaching more than 3-fold increase in comparison to their pH 7 controls (100k SEC7 and 100k PDP7, respectively), whereas P samples (100k P5.5 and 100k P7) did not show any difference (Figure 2B). Subsequently, nanoparticle-tracking analyses (NTAs) of the same samples further corroborated observations made with the flow cytometry. Particle concentration was substantially higher in all pH 5.5 samples, with the most prominent differences (more than 50-fold) observed in samples 20k P5.5 and 100k PDP5.5 (Figure 2C). Looking further into the PSD, we observed generally larger particles in acidified samples (Figure 2C). However, the 20k P7, 100k P7, and 100k P5.5 samples had fewer traceable particles. Additionally, protein concentration was much higher in pellets isolated in acidic conditions, reducing the particle/μg of protein ratio for most of the pH 5.5 samples (100k PDP5.5 being an exception) in comparison to the pH 7 controls (Supplementary Tables S1).

2.2 | Plasma acidification induces precipitation of EVs, enables better fractionation of subpopulations in DC, and improves EV:LP ratio

To support previous ELISA and flow cytometry data, the presence of additional EV markers was confirmed with western blotting (Figure 3A). Alix, TSG101, CD9, and actin were detected in all pH 5.5 samples while the same volume of control samples showed only faint bands of TSG101 in the 100k PDP7 and 100k SEC7. Among all the EV markers, only CD9 showed substantial differences in expression between PDP5.5 and SEC5.5, for both 20k and 100k samples. On the other hand, the LP marker ApoB was detectable in most of the samples, lacking only in 20k PDP5.5 and 100k PDP7 (Figure 3A). The overall differential signal expression of EV and LP markers between 20k and 100k pellets in acidic vs. neutral conditions was observed (densitometry analysis, Figure 3A and Supplementary Table S2). Albumin was abundant in all the samples, regardless of the loading volumes.

We analyzed the 20k PDP7, 20k PDP5.5, and 20k P5.5 with transmission electron microscopy (TEM) (Figure 3B). In 20k PDP7, numerous vesicle-shaped structures were observed, many of them confined within bigger multilamellar islets, which are likely to be residual platelets, or EVs with tubular morphology, as previously described [26] (Figure 3B). Following the acidification, similar structures could be seen in both 20k PDP5.5 and 20k P5.5, however, with much more impurities co-isolated in the precipitate. It is worth mentioning that the 20k P5.5 sample was diluted 4-fold, prior to preparation for TEM.

2.3 | Acidification depletes up to 61.2% of LPs in SEC and precipitates up to 20.4% of EVs from raw plasma in a single-step low-speed centrifugation

In order to assess the effect acidification would have on EVs or LPs alone, pure EVs (derived from LNCaP cells) or pure LPs (mix of HDL, LDL, and VLDL) were acidified using PBS pH 5.5. Neither the acidification of EVs nor LPs yielded any precipitate like it was the case with plasma. Thus, the samples were filtered through a SEC column, and selected SEC fractions were analyzed with ELISA (sandwich anti-CD9 for EVs, indirect anti-ApoB, and direct anti-ApoA1 for LPs) and NTA (Figure 4A, B). Acidification of pure EVs caused a shift in the elution to the earlier SEC fractions, as evidenced by the CD9 marker profile and particle concentration (Figure 4A). Nevertheless, the overall recovered particles and their PSD remained the same between the pH 7 and pH 5.5 (Figure 4A and Supplementary Figure S6A). Acidification of

capturing and anti-ApoB antibody for detection). Results are shown as the signal-to-background ratio (S/B). Additionally, the protein concentration was assessed with BCA assay. **(E)** NTA analysis was performed to estimate particle concentrations and PSD with median diameters (shown as the frequency histograms, with vertical lines representing the X50 sizes) for each of the SEC fractions. Data are presented as a mean ±SEM of at least 3 independent experiments. Statistical significance was analyzed using 2-way analysis of variance with Šídák's test for multiple comparisons (alpha = 0.05, p = .1234 [ns], 0.0332 [*], 0.0021 [**], 0.0002 [***], <0.0001 [****]). Detailed results of the statistical analysis are provided in the supplementary material. A workflow scheme was created with BioRender.com.

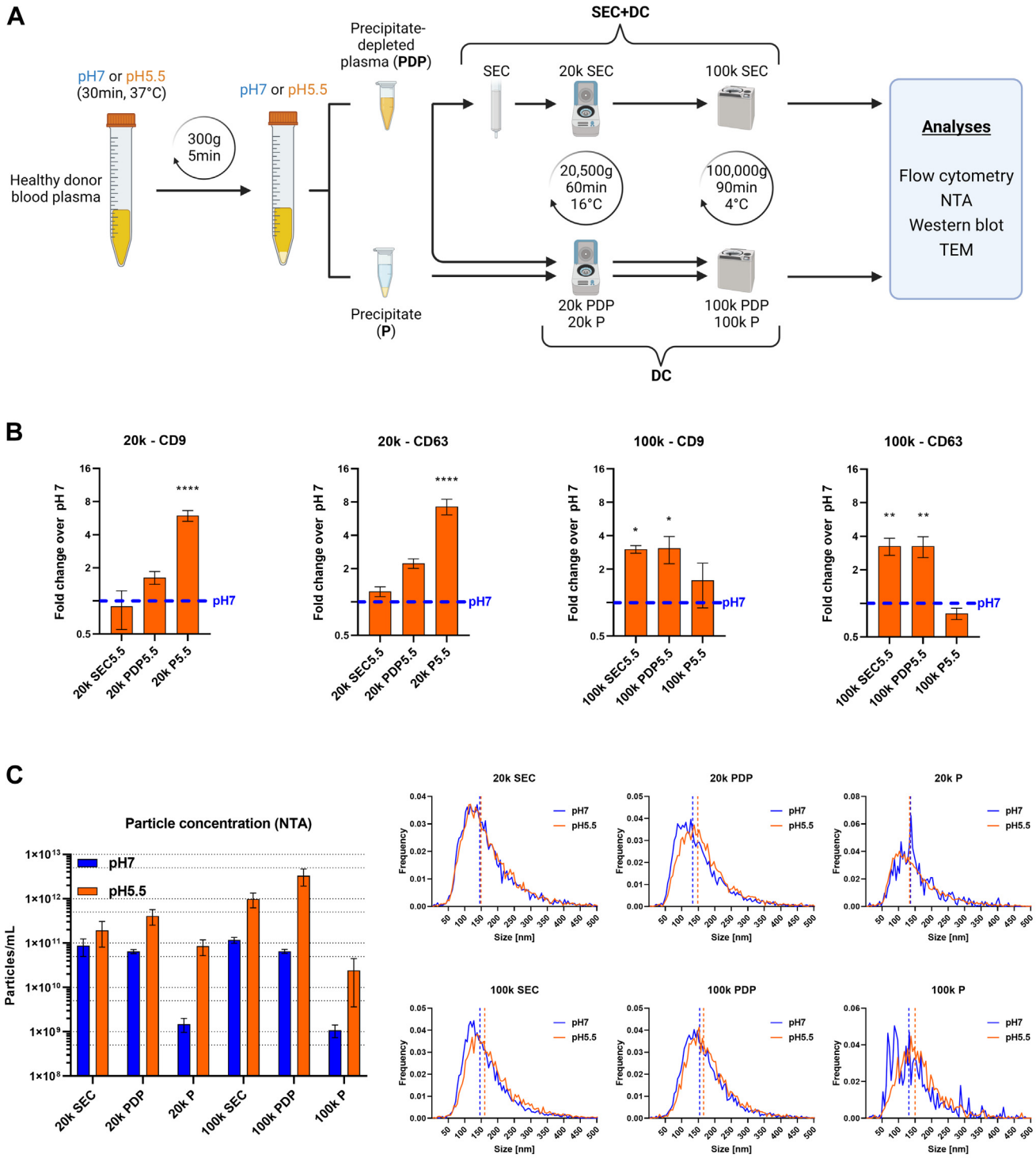

FIGURE 2 Sample fractionation with differential centrifugation (DC) in order to separate medium/large and small EVs. **(A)** SEC5.5, PDP5.5, and P5.5 samples (as well as the controls SEC7, PDP7, and P7) were subjected to DC at 20 500 *g* for 60 minutes and 100 000 *g* for 90 minutes, in order to assess the effect of acidic conditions (pH 5.5) on isolation and downstream analysis of certain subpopulations of EVs. **(B)** Pellets from both centrifugation steps (20 K and 100 K) were analyzed on CytoFLEX S flow cytometer, using fluorescently labeled anti-CD9 and anti-CD63 antibodies. Detected events were normalized to the counting beads standards included in each measurement. Final values are expressed as fold change between pH 5.5 and pH 7. **(C)** Particle concentrations (shown as the bar chart with logarithmic Y axis) and PSD with median diameters (shown as the frequency histograms with vertical lines representing the X50 sizes) were obtained with ZetaView NTA instrument. Data are presented as a mean ±SEM of 3 independent experiments. Statistical significance was analyzed using 2-way analysis of variance with Šídák's test for multiple comparisons (alpha = 0.05, p = .1234 [ns], 0.0332 [*], 0.0021 [**], 0.0002 [***], <0.0001 [****]). Detailed results of the statistical analysis, as well as the CytoFLEX S dot plots (Supplementary Figures S1 and S2), the concentration of $CD9^+$ and $CD63^+$ EVs from the repeated experiments (Supplementary Figure S3), and the histogram with violet SSC ranges of beads size standards (Supplementary Figure S4) are provided in the supplementary material. Additionally, photographs and schematic representations of the pellets obtained with DC are provided in Supplementary Figure S5. A workflow scheme was created with BioRender.com.

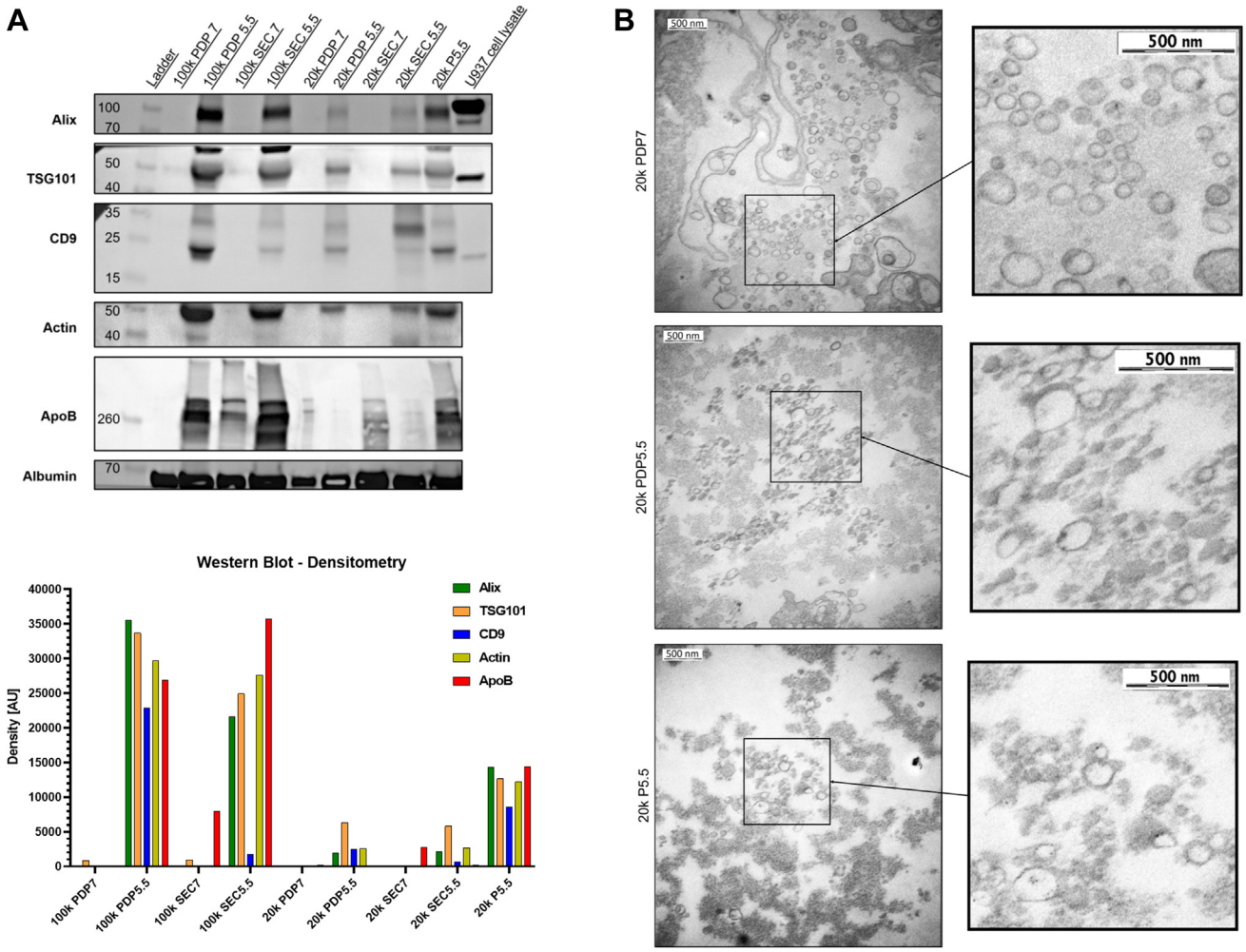

FIGURE 3 Western blot and TEM analyses of samples fractionated by DC. **(A)** Twenty and 100 k PDP and SEC samples from both pH conditions, as well as the 20 k P5.5, were analyzed with western blot for the expression of 4 common EV markers (Alix, TSG101, CD9, and actin) and 2 non-EV markers (ApoB and albumin), according to the MISEV2018 guidelines. Densitometric analysis was performed using the ImageJ software. **(B)** 20k PDP7, 20 k PDP5.5, and 20kP5.5 were also imaged with TEM in order to see the initial effect of moderate acidification on the morphology of plasma EVs, and potential co-isolates.

pure LPs showed an overall reduction of both LP markers (ApoB and ApoA1), although with much higher variability between the experiments (Figure 4B). The LP depletion in terms of particle concentration was significant, showing reduction of up to 61.2% (Figure 4B). The size of the particles was only slightly increased at pH 5.5, in the fractions 9-11 (Supplementary Figure S6B).

In additional experiments, purified EVs derived from HT29 cells were labeled with CFSE and the excess dye was removed by SEC. Fluorescent EVs (fluo-EVs) were then spiked into the plasma for the assessment of EV enrichment in the precipitate (P5.5) and the control sample (P7). There was no difference between P5.5 and P7 in terms of total protein and particle concentration, however, considerable redistribution of fluorescent events was observed in P5.5 with both fluorescent NTA (FNTA) and bulk fluorescence measurement in the plate reader (Figure 4C). After acidification, approximately 17.1%-20.4% of fluorescent EVs were recovered in P5.5 (Figure 4C). Despite having the same total particle concentration as P7, P5.5 had 11.5-fold higher concentration of fluo-EVs, demonstrating the prevalent enrichment of EVs in acidification-induced precipitate (Figure 4C).

3 | DISCUSSION

In this study, we addressed 2 main shortcomings in plasma EV preparations – low EV yield and LP co-isolation. We ultimately described moderate plasma acidification as a quick single-step precipitation method for the enrichment of plasma EVs, and as a prospective methodological amelioration of SEC or DC that could improve the yield of EVs and partially deplete LPs.

So far, it has been reported that EVs, unlike LPs, generally show greater resilience to pH changes, as they are readily isolated from biofluids spanning wider pH ranges, such as urine (from pH 4.5 up to pH 8) [3,27,28]. Acidic anticoagulants (e.g., ACD with pH 4.5) are widely adopted for blood collection in EV studies, given that a low pH

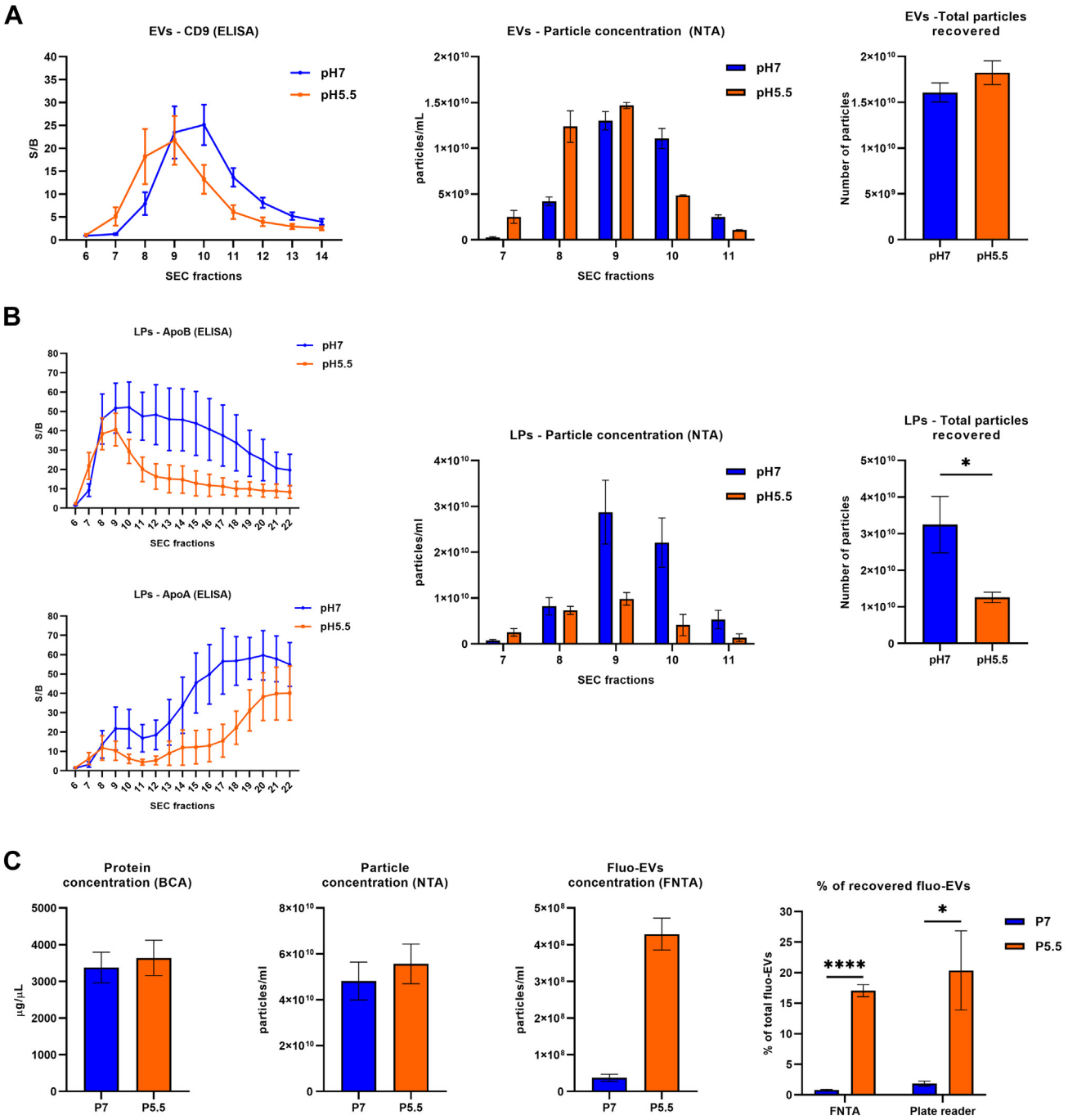

FIGURE 4 Assessing the effect of acidification on pure EVs or LPs, and quantifying the EVs recovered in the P5.5. Purified EVs (derived from LNCaP cells) or LPs (mix of HDL, LDL, and VLDL) were added to the PBS pH 5.5 and filtered through the SEC column to simulate the acidic conditions of plasma SEC purification. **(A)** The EV elution profile was assessed using the sandwich ELISA (anti-CD9 antibody for capturing and detection) and NTA. **(B)** LP elution profile was assessed using an indirect and direct ELISA (high-binding capacity 96-well plate for capturing and anti-ApoB or anti-ApoA1 antibody for detection, respectively) and NTA. ELISA results are presented as signal-to-background ratio (S/B). **(C)** Purified EVs (derived from HT29 cells) were fluorescently labeled with CFSE and spiked into the plasma samples. After acidification, the concentration of proteins, total particles, and fluo-EVs in P7 and P5.5 were measured with BCA, NTA, and FNTA, respectively. The percentages of recovered fluo-EVs in P7 and P5.5 were measured using FNTA and plate reader (FITC channel). All data are shown as the mean ±SEM of at least 3 independent experiments. Statistical significance in the percentage of recovered fluo-EVs was analyzed using unpaired parametric *t*-test, with Holm–Šídák test for multiple comparisons (2-tailed *p* value, alpha = 0.05, $p = .1234$ [ns], 0.0332 [*], 0.0021 [**], 0.0002 [***], <0.0001 [****]). Detailed results of the statistical analysis are provided in the supplementary material.

environment stabilizes platelets and prevents their activation [29–32]. Furthermore, protocols for milk EV isolation resort to acidification (pH 4.6) as a mean of removing casein contaminants and improving the purity, although, with potential adverse effects on the structural integrity of EVs [33,34]. Other studies with storage conditions and techniques for manipulating EVs in even stronger acidic environments have also been reported [35,36]. Moreover, low pH could potentially be used to increase the yield of isolated EVs [37,38]. Acidification has also been utilized for quick EV precipitation using sodium acetate at pH 4.75 [39].

The proposed mechanism of precipitation in the aforementioned study was "salting-out" caused by acetate, since hydrochloric acid did not induce precipitation at the same pH. On the other hand, our results indicate that the moderate acidification of plasma (pH 5.5) using hydrochloric acid could lead to direct precipitation by diminishing repulsive electrostatic forces and reducing the solubility of EVs and proteins. Given that EVs have net negative surface charge, the isoelectric precipitation in acidic conditions was expected [24,25]. Low-speed centrifugation (5 minutes at 300 *g*) was already sufficient to pull down up to 20.4% of EVs from acidified plasma (Figure 4C). Furthermore, the profile of EV markers in the precipitate was similar to that of the EVs obtained with much higher centrifugal force and longer processing time (Figure 3A: 20k P5.5 vs 100k PDP5.5).

Acidification significantly improved plasma EV separation by SEC and increased their sedimentation by DC (Figures 1D, 2B, and 3A). However, many proteins were co-isolated (especially in 20k P5.5), denoting one of the limitations of this method: the particles/μg of protein are mostly lower (Supplementary Table S1). Furthermore, acidification showed to be effective in LP depletion from EV preparations (Figures 1D, 3A, and 4B), supporting our initial hypothesis and earlier reports claiming that the LPs could be destabilized in acidic conditions, particularly VLDL and LPs carrying ApoB [22,23]. Our data suggest that even the smaller ApoA1-expressing HDL may be affected by acidification (Figure 4B), providing an overall higher EV:LP ratio in the downstream analyses (Figures 3A, 4A, and 4B; Supplementary Table S2).

In summary, 20k centrifugation of the pH 5.5 samples resulted in higher yield of EVs as compared with the same volume of the pH 7 samples, higher protein, and lower LP contamination, whereas the 100k centrifugation of pH 5.5 samples had even higher yield of EVs compared with the pH 7 samples, favoring less protein contamination, and a still fair EV:LP ratio (Figure 3A, Supplementary Tables S1 and S2). By cross-comparison of the pH 5.5 pellets from 20k and 100k, we could appreciate higher EV marker content in 100k samples per same amount of proteins, confirming again that the EV/μg of protein ratio was higher after 100k centrifugation, while 20k centrifugation provided better EV:LP purity (Figure 3A, Supplementary Tables S1 and S2). This may have implications in future EV biomarker studies, especially if the downstream analyses require consideration of co-isolated proteins and/or LPs.

We speculate that there was also a potential aggregation of EVs caused by acidification of plasma, since the median particle size was slightly larger in pH 5.5 samples, especially after DC. This improved the flow cytometry analyses, by clustering smaller vesicles into larger events, thus enabling them to reach the detection limit of the instrument. This was reflected in a noticeable shift of the violet SSC to the right in dot plots (Supplementary Figures S1 and S2). It is worth mentioning that the detected signal did not suffer from the swarm effect, since the serial dilution of the sample produced linear number of detected events (data not shown).

All the presented results accrue to a significant body of evidence that acid precipitation has a potential for future EV-based biomarker discoveries, in particular those of rare subpopulations relevant for certain diseases. Although coprecipitation of other plasma proteins might pose a limiting factor, it should be taken into consideration that the EV surface interactome is remarkably complex, and many entities in biofluids, such are proteins and lipoproteins in blood plasma, are predestined to associate with EVs. Previous studies have investigated the complexity and nature of such interactions, revealing that many presumed "non-EV" markers are in fact in intimate connection with the surface of EVs [19,21,40]. Whether this biological corona has significance in physiological processes, is still to be clarified. For now, it remains as a remark that bona fide EV markers might not only be molecular components of EVs built-in during their biogenesis but also other molecules that are inevitably associated later on. This should be considered in assessing novel EV-based biomarkers also in an acidification-induced precipitate, especially if the enrichment is linked to some diagnostically relevant molecules.

4 | CONCLUSION

Our study demonstrated the benefits of plasma acidification during the separation of EVs with both SEC and DC, while at the same time improving EV:LP ratio. Lowering pH to 5.5 enables higher sedimentation efficiency of EVs in commonly used DC protocols, which facilitates downstream detection and analyses by enriching EVs in lower sample volumes. At the same time, immediate precipitation occurring in plasma at pH 5.5 serves as a prospective method for simplified upstream processing, resulting in rapid recoveries of up to 20.4% of EVs. Finally, such a straightforward, resource-efficient, and high-gaining technique may have a substantial impact on ensuing biomarker research.

5 | METHODS

5.1 | Blood plasma processing

Healthy donor blood plasma pool, processed as described in Supplementary Methods, was purchased from BioIVT (Human Plasma K2EDTA; BioIVT). Prior to the experiments, the plasma was thawed and immediately centrifuged at 2500 *g*, for 15 minutes at 4 °C. Such precleared plasma was then used for EV isolation.

5.2 | Assessment of the range of moderate acidification (pH 7 to pH 5)

Precleared plasma samples were acidified until reaching pH 6, pH 5.5, and pH 5, and incubated at 37 °C for 30 minutes. The resulting precipitates (P7, P6, P5.5, and P5), were pelleted by centrifugation at 300 *g* for 5 minutes, resuspended in PBS up to 500 μL, and used for the automated western blot analyses by Wes, as described below. MiniPURE-EVs SEC columns (HansaBioMed Life Sciences) were equilibrated with appropriate PBS (pH 7, pH 6, pH 5.5, or pH 5), and 500 μL of each remaining precipitate-depleted plasma (PDP7, PDP6, PDP5.5, and PDP5) was purified, according to the manufacturer's instructions. For each pH condition, fractions containing EVs were pooled together (SEC7, SEC6, SEC5.5, and SEC5) and used in the downstream automated western blot analyses. The detailed protocol is provided in Supplementary Methods.

5.3 | Acidification and EV isolation

Precleared plasma was acidified until reaching pH 5.5, diluted with PBS of the same pH, and incubated at 37 °C for 30 minutes, followed by separation of P5.5 and PDP5.5 by low-speed centrifugation at 300 *g* for 5 minutes. As a control, pH-neutral plasma was processed in the same way. After the separation of PDP and P, EVs were isolated from 2 mL of PDP7 and PDP5.5 either by SEC, DC, or combination of the 2 (SEC+DC). PURE-EVs SEC columns (HansaBioMed Life Sciences) were equilibrated with PBS pH 7 or pH 5.5, and the purification was carried out following the manufacturer's instructions. DC consisted of 2 centrifugation steps (60 minutes at 20 500 *g* and 16 °C, and 90 minutes at 100 000 *g* and 4 °C), previously described for plasma EV isolation [21]. Precipitate samples (P7 and P5.5) were subjected to EV isolation only by DC. The detailed protocol is provided in Supplementary Methods.

5.4 | ELISA

Anti-CD9 sandwich ELISA (ExoTEST; HansaBioMed Life Sciences) was used for the analysis of EV marker expression (CD9) in SEC fractions, whereas indirect and direct ELISA in the high-binding capacity 96-well plate (Biomat) was used for the analysis of LP marker expression (ApoB and ApoA1, respectively). All samples were loaded in equal volumes (100 μL). The detailed protocol is provided in Supplementary Methods.

5.5 | BCA protein quantification

Pierce BCA Protein Assay Kit (Thermo Fisher Scientific) and Micro BCA Protein Assay Kit (Thermo Fisher Scientific) were used according to the manufacturer's instructions. Ten and 2 μL of each sample were used for protein quantification using BCA or Micro BCA assay kit, respectively. The absorbance was measured at 540 nm with GENios Pro microplate reader (Tecan Group Ltd.) and NanoDrop ND-1000 spectrophotometer (Thermo Fisher Scientific).

5.6 | Western blot

Twenty and 100k samples were analyzed for the expression of TSG101, Alix, CD9, actin, ApoB, and albumin using the western blot technique, as described in Supplementary Methods. Fourty microgram of proteins from each pH 5.5 sample was loaded onto the 4%-20% Mini-PROTEAN TGX Precast gel (Bio-Rad Laboratories), while pH 7 samples were loaded in volumes corresponding to their pH 5.5 pairs, due to the very low protein concentrations. Samples 20k P7, 100k P7, and 100k P5.5 were omitted from the analyses, as the protein concentrations were under the limit of detection by Micro BCA assay, or insufficient for the western blot analyses. Markers were selected according to the general MISEV guidelines [41]. The detailed protocol is provided in Supplementary Methods.

5.7 | Automated western blot

Pooled EV SEC fractions (SEC7, SEC6, SEC5.5, and SEC5) and precipitates (P7, P6, P5.5, and P5) from plasma samples at different pH levels (pH 7 to pH 5), 1 μL of each, were analyzed using Wes automated western blot system (Bio-Techne Protein Simple) according to the manufacturer's guidelines. All samples were analyzed for the expression of common EV marker CD9 and LP marker ApoA1. The detailed protocol is provided in Supplementary Methods.

5.8 | CytoFLEX S fluorescence analyses

Pellets from both centrifugation steps (20k and 100k) were analyzed by flow cytometry (CytoFLEX S V4-B4-R3-I2, Beckman Coulter). Five microliter of 20k samples or 2 μL of 100k samples were stained with 1 μL of antihuman CD9 PE-conjugated monoclonal antibody (Sony Biotechnology), or 1 μL antihuman CD63 PE- or PerCP/CyC5.5-conjugated monoclonal antibody (Sony Biotechnology). Unstained samples, buffer only, and dye only (buffer and fluorochrome-conjugated antibodies) were used as a control and for setting the fluorescence threshold. Sample incubation and analysis were carried out as described in Supplementary Methods.

5.9 | NTA

Two different ZetaView PMX-120 NTA instruments (Particle Metrix) were used for single-particle analyses – the one with 488 nm laser was used for all of the scatter and fluorescence analyses, except for the results in the Figure 2C, which were produced with the instrument with 520 nm laser. Both instruments were setup according to the manufacturer's guidelines, and the parameters used for 11-positions measurements were previously described [42]. The detailed protocol is provided in Supplementary Methods.

5.10 | TEM

Pelleted EVs were fixed, dehydrated, block-stained, and embedded in Taab 812 resin (Taab) as described in Supplementary Methods. After polymerization at 60 °C for 12 hours, 50-60 nm ultrathin sections were prepared using a Leica UCT ultramicrotome (Leica Microsystems) and examined by a Hitachi 7100 transmission electron microscope (Hitachi Ltd.). Electron micrographs were made by Veleta 2k x 2k MegaPixel side-mounted TEM CCD camera (Olympus). The detailed protocol is provided in Supplementary Methods.

5.11 | Acidification of purified EVs or LPs

Purified EVs from LNCaP cell line (HansaBioMed Life Sciences) were acidified by adding 100 μL of EVs to 1 mL of PBS pH 5.5. Conversely, LP mix comprising HDL, LDL (Merck Millipore), and VLDL (Athens Research & Technology), 5 μL of each, was added to 1.5 mL of PBS pH 5.5. Acidified EVs or LPS were then incubated at 37 °C for 30 minutes, followed by short centrifugation at 300 *g* for 5 minutes. As there was no precipitation like in plasma, 1 mL of sample was purified with PURE EVs SEC column, previously equilibrated with PBS pH 5.5. Fractions of 500 μL were collected for downstream analyses (ELISA, NTA), as described in the previous chapters. The same procedure was performed with the control samples at pH 7.

5.11 | Fluorescent EVs spike-in experiments

Purified EVs from HT29 cell line (HansaBioMed Life Sciences) were labeled with 50 μM CFSE (Thermo Fisher Scientific), following the protocol previously described [42]. After washing the excess of dye using miniPURE-EVs SEC column (HansaBioMed Life Sciences), 130 μL of purified fluo-EVs were spiked into 2 mL of plasma, and the acidification was performed. Upon separation, PDP5.5 and P5.5 were analyzed with NTA, FNTA, and plate reader to estimate the redistribution of fluo-EVs, and the protein concentration was determined using BCA. As a control, non-acidified plasma was spiked with the same amount of fluo-EVs to obtain PDP7 and P7. Nonspiked plasma (2 mL of plasma + 130 μL of PBS), and subsequently obtained PDP5.5 and P5.5 (as well as the PDP7 and P7) were used as a control for autofluorescence. Detailed description of the method, calculation of fluorescent particles, and their redistribution in P5.5 and P7 are provided in Supplementary Methods.

ACKNOWLEDGMENTS

This work was supported by following funding programmes: European Union's Horizon 2020 research and innovation programme under the grant agreement number H2020-MSCA-ITN-2017-722148 (TRAIN EV); European Regional Development Fund Enterprise Estonia's Applied Research Program under the grant agreement number 2014-2020.4.02.21-0398 (EVREM), National Scientific Research Program of Hungary (OTKA) NVKP_16-1-2016-0017, Higher Education Institutional Excellence Program – Therapeutic development, Ministry for National Economy of Hungary under the grant number VEKOP-2.3.2-16-2016-00002, VEKOP-2.3.3-15-2017-00016, European Union's Horizon 2020 research and innovation program under the grant agreement number 739593, and the grant TKP-2021-Terapias-EGA-23.

AUTHOR CONTRIBUTIONS

D.M. and D.K. contributed equally to this work. Conceptualization, D.M. and N.Z.; Methodology; D.M. and D.K.; Data Curation, D.M., D.K. and A.K.; Formal Analysis, D.M., D.K. and A.K.; Validation, D.M., D.K., E.I.B. and N.Z.; Writing—Original Draft Preparation, D.M. and D.K.; Writing—Review and Editing N.Z., E.I.B., A.K. and K.K.; Supervision, N.Z., E.I.B. and K.K. All authors read and approved the final manuscript.

DECLARATION OF COMPETING INTERESTS

There are no competing interests to disclose.

TWITTER

Danilo Mladenović @DanMladenovic

REFERENCES

[1] Yáñez-Mó M, Siljander PR, Andreu Z, Zavec AB, Borràs FE, Buzas EI, Buzas K, Casal E, Cappello F, Carvalho J, Colás E, Cordeiro-da Silva A, Fais S, Falcon-Perez JM, Ghobrial IM, Giebel B, Gimona M, Graner M, Gursel I, Gursel M, et al. Biological properties of extracellular vesicles and their physiological functions. *J Extracell Vesicles*. 2015;4:27066.

[2] Palviainen M, Saraswat M, Varga Z, Kitka D, Neuvonen M, Puhka M, Joenväärä S, Renkonen R, Nieuwland R, Takatalo M, Siljander PRM. Extracellular vesicles from human plasma and serum are carriers of extravesicular cargo-Implications for biomarker discovery. *PLoS One*. 2020;15:e0236439.

[3] Lozano-Ramos I, Bancu I, Oliveira-Tercero A, Armengol MP, Menezes-Neto A, Del Portillo HA, Lauzurica-Valdemoros R, Borràs FE. Size-exclusion chromatography-based enrichment of extracellular vesicles from urine samples. *J Extracell Vesicles*. 2015;4:27369.

[4] Chiasserini D, van Weering JR, Piersma SR, Pham TV, Malekzadeh A, Teunissen CE, de Wit H, Jiménez CR. Proteomic analysis of cerebrospinal fluid extracellular vesicles: a comprehensive dataset. *J Proteom*. 2014;106:191–204.

[5] Iwai K, Minamisawa T, Suga K, Yajima Y, Shiba K. Isolation of human salivary extracellular vesicles by iodixanol density gradient ultracentrifugation and their characterizations. *J Extracell Vesicles*. 2016;5:30829.

[6] Ostenfeld MS, Jensen SG, Jeppesen DK, Christensen LL, Thorsen SB, Stenvang J, Hvam ML, Thomsen A, Mouritzen P, Rasmussen MH, Nielsen HJ, Ørntoft TF, Andersen CL. miRNA profiling of circulating EpCAM(+) extracellular vesicles: promising biomarkers of colorectal cancer. *J Extracell Vesicles*. 2016;5:31488.

[7] Rikkert LG, Beekman P, Caro J, Coumans FAW, Enciso-Martinez A, Jenster G, Le Gac S, Lee W, van Leeuwen TG, Loozen GB, Nanou A, Nieuwland R, Offerhaus HL, Otto C, Pegtel DM, Piontek MC, van der Pol E, de Rond L, Roos WH, Schasfoort RBM, et al. Cancer-ID: toward identification of cancer by tumor-derived extracellular vesicles in blood. *Front Oncol*. 2020;10:608.

[8] Zhou B, Xu K, Zheng X, Chen T, Wang J, Song Y, Shao Y, Zheng S. Application of exosomes as liquid biopsy in clinical diagnosis. *Signal Transduct Target Ther*. 2020;5:144.

[9] Vagner T, Spinelli C, Minciacchi VR, Balaj L, Zandian M, Conley A, Zijlstra A, Freeman MR, Demichelis F, De S, Posadas EM, Tanaka H, Di Vizio D. Large extracellular vesicles carry most of the tumour

DNA circulating in prostate cancer patient plasma. *J Extracell Vesicles*. 2018;7:1505403.
[10] Sharma P, Ludwig S, Muller L, Hong CS, Kirkwood JM, Ferrone S, Whiteside TL. Immunoaffinity-based isolation of melanoma cell-derived exosomes from plasma of patients with melanoma. *J Extracell Vesicles*. 2018;7:1435138.
[11] Nawaz M. Mining extracellular vesicles for clinically relevant noninvasive diagnostic biomarkers in cancer. In: Farah F, ed. *Novel Implications of Exosomes in Diagnosis and Treatment of Cancer and Infectious Diseases*. Rijeka: IntechOpen; 2017. Ch. 6. https://doi.org/10.5772/intechopen.69406. [accessed May 19, 2022].
[12] Li Y, He X, Li Q, Lai H, Zhang H, Hu Z, Li Y, Huang S. EV-origin: enumerating the tissue-cellular origin of circulating extracellular vesicles using exLR profile. *Comput Struct Biotechnol J*. 2020;18:2851–9.
[13] Karimi N, Cvjetkovic A, Jang SC, Crescitelli R, Hosseinpour Feizi MA, Nieuwland R, Lötvall J, Lässer C. Detailed analysis of the plasma extracellular vesicle proteome after separation from lipoproteins. *Cell Mol Life Sci*. 2018;75:2873–86.
[14] Johnsen KB, Gudbergsson JM, Andresen TL, Simonsen JB. What is the blood concentration of extracellular vesicles? Implications for the use of extracellular vesicles as blood-borne biomarkers of cancer. *Biochim Biophys Acta Rev Cancer*. 2019;1871:109–16.
[15] Simonsen JB. What are we looking at? extracellular vesicles, lipoproteins, or both? *Circ Res*. 2017;121:920–2.
[16] Li K, Wong DK, Luk FS, Kim RY, Raffai RL. Isolation of plasma lipoproteins as a source of extracellular RNA. *Methods Mol Biol*. 2018;1740:139–53.
[17] Michell DL, Vickers KC. Lipoprotein carriers of microRNAs. *Biochim Biophys Acta*. 2016;1861:2069–74.
[18] Sumenkova DV, Polyakov LM, Panin LE. Plasma lipoproteins as a transport form of extracellular DNA. *Bull Exp Biol Med*. 2013;154:622–3.
[19] Buzás EI, Tóth EÁ, Sódar BW, Szabó-Taylor KÉ. Molecular interactions at the surface of extracellular vesicles. *Semin Immunopathol*. 2018;40:453–64.
[20] Busatto S, Yang Y, Walker SA, Davidovich I, Lin WH, Lewis-Tuffin L, Anastasiadis PZ, Sarkaria J, Talmon Y, Wurtz G, Wolfram J. Brain metastases-derived extracellular vesicles induce binding and aggregation of low-density lipoprotein. *J Nanobiotechnol*. 2020;18:162.
[21] Sódar BW, Kittel Á, Pálóczi K, Vukman KV, Osteikoetxea X, Szabó-Taylor K, Németh A, Sperlágh B, Baranyai T, Giricz Z, Wiener Z, Turiák L, Drahos L, Pállinger É, Vékey K, Ferdinandy P, Falus A, Buzás EI. Low-density lipoprotein mimics blood plasma-derived exosomes and microvesicles during isolation and detection. *Sci Rep*. 2016;6:24316.
[22] Guha M, Gursky O. Human plasma very low-density lipoproteins are stabilized by electrostatic interactions and destabilized by acidic pH. *J Lipids*. 2011;2011:493720.
[23] Fernández-Higuero JA, Benito-Vicente A, Etxebarria A, Milicua JCG, Ostolaza H, Arrondo JLR, Martín C. Structural changes induced by acidic pH in human apolipoprotein B-100. *Sci Rep*. 2016;6:36324.
[24] Nguyen DB, Tran HT, Kaestner L, Bernhardt I. The relation between extracellular vesicles released from red blood cells, their cargo, and the clearance by macrophages. *Front Physiol*. 2022;13:783260.
[25] Midekessa G, Godakumara K, Ord J, Viil J, Lättekivi F, Dissanayake K, Kopanchuk S, Rinken A, Andronowska A, Bhattacharjee S, Rinken T, Fazeli A. Zeta potential of extracellular vesicles: toward understanding the attributes that determine colloidal stability. *ACS omega*. 2020;5:16701–10.
[26] Arraud N, Linares R, Tan S, Gounou C, Pasquet JM, Mornet S, Brisson AR. Extracellular vesicles from blood plasma: determination of their morphology, size, phenotype and concentration. *J Thromb Haemost*. 2014;12:614–27.
[27] Dong L, Zieren RC, Horie K, Kim CJ, Mallick E, Jing Y, Feng M, Kuczler MD, Green J, Amend SR, Witwer KW, de Reijke TM, Cho YK, Pienta KJ, Xue W. Comprehensive evaluation of methods for small extracellular vesicles separation from human plasma, urine and cell culture medium. *J Extracell Vesicles*. 2020;10:e12044.
[28] Bono MJ, Reygaert WC. Urinary tract infection. In: *StatPearls. Treasure Island (FL)*. StatPearls Publishing; 2022.
[29] Aatonen M, Valkonen S, Böing A, Yuana Y, Nieuwland R, Siljander P. Isolation of platelet-derived extracellular vesicles. In: Hill AF, ed. *Exosomes and microvesicles: methods and protocols*. New York, NY: Springer New York; 2017:177–88.
[30] György B, Pálóczi K, Kovács A, Barabás E, Bekő G, Várnai K, Pállinger É, Szabó-Taylor K, Szabó TG, Kiss AA, Falus A, Buzás EI. Improved circulating microparticle analysis in acid-citrate dextrose (ACD) anticoagulant tube. *Thromb. Res*. 2014;133:285–92.
[31] Pignatelli P, Pulcinelli FM, Ciatti F, Pesciotti M, Sebastiani S, Ferroni P, Gazzaniga PP. Acid citrate dextrose (ACD) formula as a new anticoagulant in the measurement of in vitro platelet aggregation. *J Clin Lab Anal*. 1995;9:138–40.
[32] Green FW Jr, Kaplan MM, Curtis LE, Levine PH. Effect of acid and pepsin on blood coagulation and platelet aggregation. A possible contributor to prolonged gastroduodenal mucosal hemorrhage. *Gastroenterology*. 1978;74:38–43.
[33] Rahman MdM, Shimizu K, Yamauchi M, Takase H, Ugawa S, Okada A, Inoshima Y. Acidification effects on isolation of extracellular vesicles from bovine milk. *PLOS ONE*. 2019;14:e0222613.
[34] Yamauchi M, Shimizu K, Rahman M, Ishikawa H, Takase H, Ugawa S, Okada A, Inoshima Y. Efficient method for isolation of exosomes from raw bovine milk. *Drug Dev Ind Pharm*. 2019;45:359–64.
[35] Jeyaram A, Lamichhane TN, Wang S, Zou L, Dahal E, Kronstadt SM, Levy D, Parajuli B, Knudsen DR, Chao W, Jay SM. Enhanced loading of functional miRNA cargo via pH gradient modification of extracellular vesicles. *Mol Ther*. 2020;28:975–85.
[36] Cheng Y, Zeng Q, Han Q, Xia W. Effect of pH, temperature and freezing-thawing on quantity changes and cellular uptake of exosomes. *Protein Cell*. 2019;10:295–9.
[37] Ban JJ, Lee M, Im W, Kim M. Low pH increases the yield of exosome isolation. *Biochem Biophys Res Commun*. 2015;461:76–9.
[38] Zhao Y, Chen K, Li H, Wu H. Effect of pH on the isolation of urinary exosome. *Int Urol Nephrol*. 2017;49:165–9.
[39] Brownlee Z, Lynn KD, Thorpe PE, Schroit AJ. A novel "salting-out" procedure for the isolation of tumor-derived exosomes. *J Immunol Methods*. 2014;407:120–6.
[40] Tóth EÁ, Turiák L, Visnovitz T, Cserép C, Mázló A, Sódar BW, Försönits AI, Petővári G, Sebestyén A, Komlósi Z, Drahos L, Kittel Á, Nagy G, Bácsi A, Dénes Á, Gho YS, Szabó-Taylor KÉ, Buzás EI. Formation of a protein corona on the surface of extracellular vesicles in blood plasma. *J Extracell Vesicles*. 2021;10:e12140.
[41] Théry C, Witwer KW, Aikawa E, Alcaraz MJ, Anderson JD, Andriantsitohaina R, Antoniou A, Arab T, Archer F, Atkin-Smith GK, Ayre DC, Bach JM, Bachurski D, Baharvand H, Balaj L, Baldacchino S, Bauer NN, Baxter AA, Bebawy M, Beckham C, et al. Minimal information for studies of extracellular vesicles 2018 (MISEV2018): a position statement of the International Society for Extracellular Vesicles and update of the MISEV2014 guidelines. *J Extracell Vesicles*. 2018;7:1535750.
[42] Fortunato D, Mladenović D, Criscuoli M, Loria F, Veiman KL, Zocco D, Koort K, Zarovni N. Opportunities and pitfalls of fluorescent labeling methodologies for extracellular vesicle profiling on high-resolution single-particle platforms. *Int J Mol Sci*. 2021:22.

SUPPLEMENTARY MATERIAL

The online version contains supplementary material available at https://doi.org/10.1016/j.jtha.2023.01.007